

This article was downloaded by:

On: 22 January 2011

Access details: *Access Details: Free Access*

Publisher *Taylor & Francis*

Informa Ltd Registered in England and Wales Registered Number: 1072954 Registered office: Mortimer House, 37-41 Mortimer Street, London W1T 3JH, UK



## The Journal of Adhesion

Publication details, including instructions for authors and subscription information:

<http://www.informaworld.com/smpp/title~content=t713453635>

### Kinetics of Adhesion Interaction of Polyolefins with Metals under Conditions of Contact Thermooxidation. 1. Oxidation Kinetics and Change of Peel Strength

M. Kalnins<sup>a</sup>; J. Malers<sup>a</sup>

<sup>a</sup> Institute of Polymer Materials, Riga Technical University, Latvia

**To cite this Article** Kalnins, M. and Malers, J.(1995) 'Kinetics of Adhesion Interaction of Polyolefins with Metals under Conditions of Contact Thermooxidation. 1. Oxidation Kinetics and Change of Peel Strength', *The Journal of Adhesion*, 50: 2, 83 – 102

**To link to this Article:** DOI: 10.1080/00218469508014360

**URL:** <http://dx.doi.org/10.1080/00218469508014360>

PLEASE SCROLL DOWN FOR ARTICLE

Full terms and conditions of use: <http://www.informaworld.com/terms-and-conditions-of-access.pdf>

This article may be used for research, teaching and private study purposes. Any substantial or systematic reproduction, re-distribution, re-selling, loan or sub-licensing, systematic supply or distribution in any form to anyone is expressly forbidden.

The publisher does not give any warranty express or implied or make any representation that the contents will be complete or accurate or up to date. The accuracy of any instructions, formulae and drug doses should be independently verified with primary sources. The publisher shall not be liable for any loss, actions, claims, proceedings, demand or costs or damages whatsoever or howsoever caused arising directly or indirectly in connection with or arising out of the use of this material.

# Kinetics of Adhesion Interaction of Polyolefins with Metals under Conditions of Contact Thermooxidation.

## 1. Oxidation Kinetics and Change of Peel Strength

M. KALNINS and J. MALERS

*Institute of Polymer Materials, Riga Technical University, Riga LV - 1048, Latvia*

*(Received June 27, 1994; in final form December 8, 1994)*

The kinetics of contact thermooxidation (CTO) of a polyethylene layer on a steel surface in connection with the change of peel strength ( $A$ ) under conditions of free access of oxygen through the polymeric layer was studied. The CTO parameters (oxygen uptake, carbon dioxide evolution, change of carbonyl group content, change of the weight of the layer) and the change in the values of  $A$  were found to be kinetically interrelated. The dependence of the rate of change of individual CTO parameters and the magnitude of  $A$  on the thickness of the layer being oxidized and temperature can be described by a simple equation. The analysis of constants in this equation allows one to estimate the catalytic effect of the substrate in CTO. The dependence of experimental determined  $A$  values on contact time can be satisfactorily described by a simple expression based on the assumption that the magnitudes of  $A$  are controlled by two main competitive processes: the accumulation of oxygen-containing groups and oxidative cross-linking, causing the increase of  $A$  values, and reactions of oxidative destruction causing the decrease in  $A$ .

**KEY WORDS** polyethylene; steel; adhesion interaction; contact thermooxidation; peel strength; weak boundary layer.

### 1. INTRODUCTION

The process of adhesion between polyolefins and metals due to direct contact of the molten polymer and the metal surface leads to the formation of a cohesively-weak polymeric boundary layer which appears to be the most unstable link in the system. Adhesive joints undergo fracture invariably in the adhesive<sup>1,2</sup> (except the process of fracture under the action of highly polar liquids);<sup>3</sup> a fracture front usually lies no less than 10 nm from the interface. The boundary layer is characterized by a low degree of order and great content of low molecular weight compounds and impurities.<sup>4,5</sup> It is a direct manifestation of the concept of a weak boundary layer. The reasons for formation of such layers was proposed by the late J. J. Bikerman.<sup>6</sup>

A large body of experimental evidence surveyed in References 7 and 8 reveals that the cohesive properties of polymeric boundary layers are defined by the contact thermooxidation (CTO) conversions in the polymer, catalyzed by metal surface com-

pounds (particularly such transient valence metals as Fe, Cu, etc.) during thermal contact.\* The CTO process can involve oxygen having been captured at the interface in the initial stages of contact, oxygen which diffuses through the polymeric layer and oxygen which is adsorbed or chemisorbed by the metal surface oxide.<sup>10</sup> In the absence of CTO extremely weak boundary layers develop.<sup>10</sup>

The purpose of our study was to establish quantitative relationships between CTO parameters and the changes in the strength of adhesive joints.

Symbols for the parameters are summarized in Table I.

The conditions of contact under which atmospheric oxygen diffuses through the layer of molten polymer are of special interest. In this case, the oxygen concentration gradient (and, consequently, the gradient of thermooxidative conversions) through the thickness of a layer must be determined both by diffusion kinetics and oxygen polymer interaction.

In the stationary stage of the oxidation process ( $dc_{ox}(x)/dt = 0$ ), the expression for oxygen concentration gradient,  $c_{ox}(x)$ , in the polymer layer of thickness,  $b$ , can be derived by a joint solution of diffusion (Fick's second law) and oxygen addition rate (first-order for oxygen) equations<sup>11,12</sup> assuming that  $dc_{ox}(x)/dx|_{x=b} = 0$  (where  $x$  is a point coordinate within the polymeric layer away from the contact surface with the environment). The expression takes the form:

$$c_{ox}(x) = \frac{c_{ox}|_{x=0} \cosh [k^*(b-x)]}{\cosh (k^*b)} \quad (1)$$

$k^* = (k/D)^{1/2}$ , where  $k$  is the rate constant for oxygen consumption and  $D$  is oxygen diffusion coefficient.

TABLE I  
List of symbols for main parameters

Parameter	Symbol
Thickness of polymer layer	$b$
Distance from the interface in the bulk of adhesive	$x$ ( $0 < x < b$ )
Rate constant for oxygen consumption by polymer	$k$
Oxygen diffusion coefficient in polymer layer	$D$
<i>Parameters which characterize contact oxidation and adhesion:</i>	$P$
Content of oxygen chemisorbed by polymer layer	$c_{ox}$
Amount of carbon dioxide released	$c_{cd}$
Change in weight of the polymer layer	$\Delta m$
Content of carbonyl groups (optical density of IR absorption)	$D_{cg}^*$
Peel strength of adhesive joints	$A$
Rate of change of parameters	$\dot{P} = dP/dt$

\* The results of the early studies of the role of CTO in polyolefin-metal adhering systems are also summarized in Reference 9.

Oxygen uptake rate per unit volume of the oxidizing polymer layer can be expressed as:

$$\dot{c}_{\text{ox}}(b) = b^{-1} \int_{x=0}^{x=b} k c_{\text{ox}}(x) dx \quad (2)$$

Substituting (1) into (2) and integrating we obtain:

$$\dot{c}_{\text{ox}}(b) = \frac{c_{\text{ox}}|_{x=0} k \tanh(k^* b)}{k^* b} \quad (3)$$

At small magnitudes of  $b$  ( $k^* b < 0.1$ ),  $\tanh(k^* b) \cong k^* b$  and  $\dot{c}_{\text{ox}}(b) = (c_{\text{ox}}|_{x=0}) k = \text{constant}$ . Below the critical magnitude of thickness ( $b_{\text{crit}} \cong 0.1 k^{*-1}$ )  $b$ , oxidation occurs in the kinetic region.

## 2. EXPERIMENTAL DETAILS

### 2.1. Materials

Unstabilized low-density polyethylene of trade mark 108-02-20 (obtained from Novopolock Chemical Enterprises) with the following characteristics was used: density-0.919 g/cm<sup>3</sup>, average values of molecular weight ( $M_n = 31200$ ,  $M_w = 36500$ ,  $M_n = 19500$ ), degree of branching-4.5 (number of tertiary-substituted C atoms per 100 C atoms of chain); melting temperature-378 K, temperature of intensive oxidation - 488 K (both according to DTA data); yield strength in tension-9.4 MPa; tensile strength-18.2 MPa, relative elongation at break-5.6, specific energy of break-84.6 MPa (all at room temperature and deformation rate 50 mm/min.).

A 70  $\mu\text{m}$  thick steel foil (approximately corresponding to the USA AJS 1010 steel) was used as a substrate, whereas Teflon film was used as an inert substrate which does not exert an influence on CTO.

### 2.2. Steel Surface Preparation

The steel surface was subjected to electro-chemical degreasing in an alkaline solution (composition in g/l:  $\text{Na}_3\text{PO}_4$ -60,  $\text{Na}_2\text{CO}_3$ -30,  $\text{NaOH}$ -15) at temperature 343-363 K and current density 10 A/dm<sup>2</sup> as a cathode for 2.5 min., then as an anode for 0.5 min. Specimens were rinsed in hot (363 K) distilled water and then dried in a filtered warm (353 K) air flow. Steel specimens were kept in a desiccator over dehydrated  $\text{CaCl}_2$  for no more than 24 hours before use. The value of the wetting angle of the prepared steel surface by water was less than 8-10°.

### 2.3. Preparation of Polymeric Films

Films of thickness 50-500  $\mu\text{m}$  were prepared by hot pressing at a temperature of 408 K and pressure of 40 KPa for 2.5 min. between Teflon films. Specimens were cooled to

room temperature between steel plates (average rate of cooling - about  $1^{\circ}\text{C}/\text{sec.}$ ), then rinsed with acetone, dried in a warm air flow and stored in the desiccator.

#### 2.4. Preparation of Samples of Adhering Systems

Laminated polymer-steel and polymer-Teflon samples were made. The polymer films were bonded with the substrate by hot-pressing at 393 K under the pressure of 40 kPa for 30 sec. in vacuum (for the purpose of excluding the effect of oxygen being entrapped in the pores of the substrate surface).

#### 2.5. Studies of Kinetics of Thermooxidation

The kinetics of absorption of atmospheric oxygen and release of carbon dioxide were studied directly, in a closed circulating system using a "Dynamoxmeter" AS - 112<sup>13</sup> at constant temperature, on polymer-substrate-polymer samples of dimensions  $18 \times 100$  mm coiled into a helix. The amount of oxygen,  $c_{\text{ox}}$ , being absorbed was determined volumetrically and the amount of released carbon dioxide,  $c_{\text{cd}}$ , was determined conductometrically both in mmoles per gram of the polymer (standard deviation, less than 5%).

The dependence of  $c_{\text{ox}}$  on contact time ( $t$ ) characterizes generally the kinetics of oxidation; the function of  $c_{\text{cd}}(t)$  - the kinetics of oxidative destruction. The change in weight of the oxidizing polymer layer,  $\Delta m(t)$  (in g per gram of polymer), was studied gravimetrically by derivatograph (F. Paulik, I. Paulik and I. Erdei system, Hungary) at constant temperature (laminated polymer-substrate-polymer specimens of dimensions  $25 \times 115$  mm coiled into a helix); standard deviation, 6%. Time curves of parameters  $c_{\text{ox}}$ ,  $c_{\text{cd}}$  and  $\Delta m$  were recorded automatically.

The kinetics of accumulation of carbonyl groups in the oxidizing polymer layer was evaluated by infra-red spectroscopy (spectrophotometers IKS-22 and IR-75). The laminated polymer-substrate specimens after contact in the air for a definite time at the fixed temperature were debonded using an electrolytic method (a kind of cathodic delamination). The specimen served as a cathode in  $\text{Na}_2\text{CO}_3$  aqueous solution (2%) with current density  $2\text{A}/\text{dm}^2$ . Interfacial debonding of the polymer film occurred.<sup>3</sup> IR spectra for adhesive films of thickness  $50\ \mu\text{m}$  (thicker films were repressed at 403 K under pressure 40 kPa for 1 min.) were obtained. The ratio ( $D_{\text{cg}}^*$ ) of values of the optical density of carbonyl group absorption (region  $1710\text{--}1740\ \text{cm}^{-1}$ ), and the optical density of absorption in the region  $4350\ \text{cm}^{-1}$  (internal standard) was determined (standard deviation was about 8–10%).

#### 2.6. Evaluation of Peel Strength of Adhesive Joints

The peel strength,  $A$ , polymer-metal laminated specimens was determined (tensile machine ZT-20, at a cross head rate of  $0.8\ \text{mm}/\text{s}$  at room temperature); standard deviation: 10–15%. In all cases the cohesive failure mode (fracture in the boundary layer of polymer) occurred. (The thickness of the residual layer of polymer on the metal surface was determined by reactive (pyrolytic) gas chromatography<sup>2</sup> and averaged 10 nm.). Thus, the peel strength values in all cases characterized the energy necessary to cause the fracture through boundary layer of adhesive.

Constant bond line thickness (500  $\mu\text{m}$ ) was provided by welding on an extra PE layer (at 473 K for 5 s under a pressure of 40 kPa). The absence of significant changes in strength-deformation characteristics of the adhesive layer during the process was established in advance (by comparison of peel strength values of adhesive joints with adhesive layer prepared with and without welding).

The size of the data points on the figures corresponds to the respective error bars for the measurements.

### 3. RESULTS AND DISCUSSION

Typical curves of variation of some of the determined parameters  $P$  (see Table I), with contact time,  $t$ , and the basic kinetic characteristics estimated from these curves are schematically shown in Figure 1 and also some experimental curves in Figure 2. Values of the basic kinetic parameters at different contact temperature,  $T$ , and thickness of adhesive layer,  $b$ , are presented in Table II. As was expected, these values are higher for contact oxidation on the steel surface due to its catalytic effect.

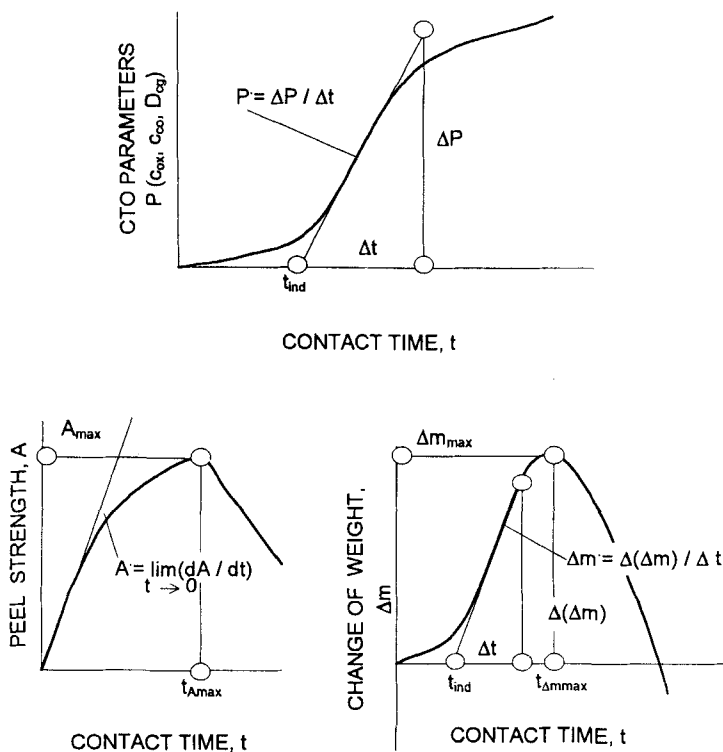


FIGURE 1 The typical shape of contact time,  $t$ , curves of parameters,  $P$ , which characterize contact oxidation of polyethylene and strength of polyethylene-steel adhesive joints and kinetic characteristics estimated therefrom.

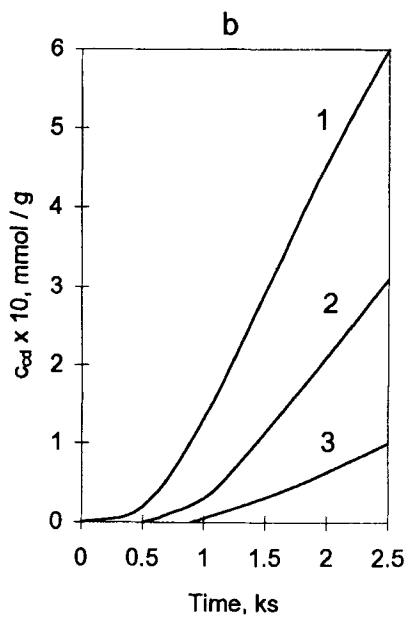
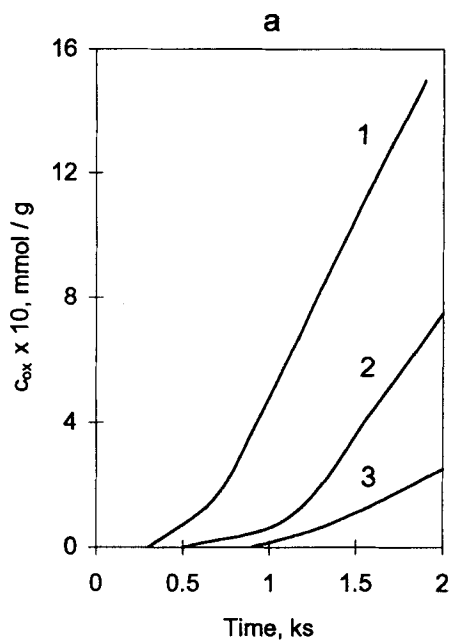


FIGURE 2 Examples of experimental curves  $P(t)$ : oxygen uptake,  $c_{ox}$  (a); release of carbon dioxide,  $c_{cd}$  (b); content of carbonyl groups,  $D^*_{c_9}$  (c); change in weight of the polymer layer,  $\Delta m$  (d); thickness of layer,  $b$  ( $\mu\text{m}$ ): 1–50, 2–100, 3–300; contact temperature, 448 K.

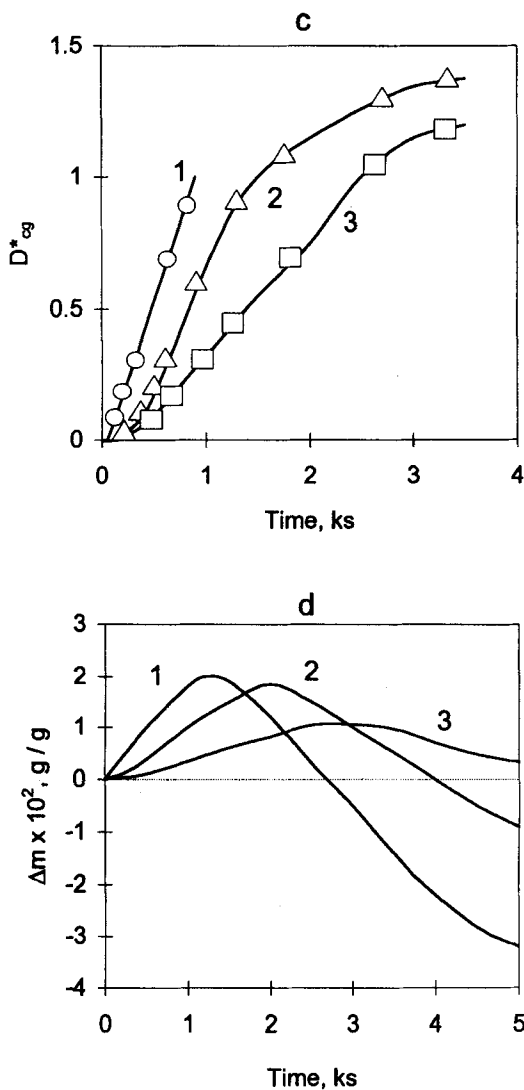


FIGURE 2 (Continued)

There is almost a linear relationship between different rate parameters, corresponding to certain  $T$  and  $b$  values. The function  $\dot{c}_{cd}(\dot{c}_{ox})$ , as an example, is presented in Figure 3. The number of moles of evolved  $\text{CO}_2$  per mole of oxygen uptake ( $n_{cd} = \dot{c}_{cd}/\dot{c}_{ox}$ ) during contact oxidation on the Teflon and steel surface are 0.16 and 0.25, respectively, *i.e.* catalysis of contact oxidation is accompanied by an increase of the yield of oxidative destruction.

The reduction of  $A$  and  $\Delta m$  values after having reached maximum (see Figs. 1, 2d and 7) is determined by the prevailing thermooxidative destruction. Therefore, the values



TABLE II  
Kinetic parameters of contact oxidation ( $\dot{c}_{ox} \times 10^4$ ,  $\dot{c}_{cd} \times 10^4$ ,  $(\text{mmol/g})\text{s}^{-1}$ ;  $\dot{D}_{eg}^* \times 10^4$ ,  $s^{-1}$ ;  $\Delta\dot{m} \times 10^6$ , mass parts  $s^{-1}$ ) and of peel strength,  $A$ , variation ( $A$ ,  $(\text{N/m})\text{s}^{-1}$ ) at various contact temperatures,  $T$ , and thickness of polymer layer,  $b$  (numerator-contact oxidation on steel surface, denominator - on Teflon);  $t$  values in ks,  $t_{ind}$ -inhibition period (see Fig. 1)

T, K	b, $\mu\text{m}$	$c_{ox}$		$c_{cd}$		$\dot{D}_{eg}^*$		$\Delta\dot{m}$		A	
		$\dot{c}_{ox}$	$t_{ind}$	$\dot{c}_{cd}$	$t_{ind}$	$\dot{D}_{eg}^*$	$t_{ind}$	$\Delta\dot{m}$	$t_{\Delta\dot{m}max}$	$t_{ind}$	$t_{Amax}$
423	0*	5.7/2.0		1.4/0.32		6.0		9.4			9.4
	50	4.6/1.8	1.6/4.0	1.1/0.3	1.4/3.6	5.5	0.5	6.7	0.4	0.4	8.9
	100	3.1/1.5	2.4/4.5	0.8/0.25	2.1/4.0	4.6	0.6	4.0	0.5	0.5	3.7
448	300	1.1/0.7	2.5/5.4	0.3/0.11	2.2/4.9	2.0	0.6	1.4	0.6	0.6	3.7
	0	15.0/7.9		3.9/1.2		13.9		24.0			16.1
	50	11.0/7.0	0.6/1.0	3.0/1.1	0.6/0.9	12.7	0.1	16.3	1.4	0	15.3
473	100	-7.5/5.3	1.0/1.4	1.0/0.9	0.9/1.3	10.1	0.3	9.5	2.1	0.15	13.1
	300	2.6/2.0	1.1/1.7	0.7/0.3	1.0/1.5	4.2	0.3	3.2	3.0	0.3	6.3
	0	34.9/28.3	4.5	8.7		31.1		55.6			28.1
483	50	26.0/22.6	0.27/0.32	6.5/3.6	0.24/0.29	27.8	0.08	36.2	0.21	0	26.2
	100	16.0/14.9	0.48/0.49	3.8/2.5	0.43/0.44	21.6	0.1	20.4	0.23	0	22.3
	300	5.5/5.2	0.60/0.60	1.4/0.8	0.54/0.53	8.6	0.1	6.9	0.44	0	10.3

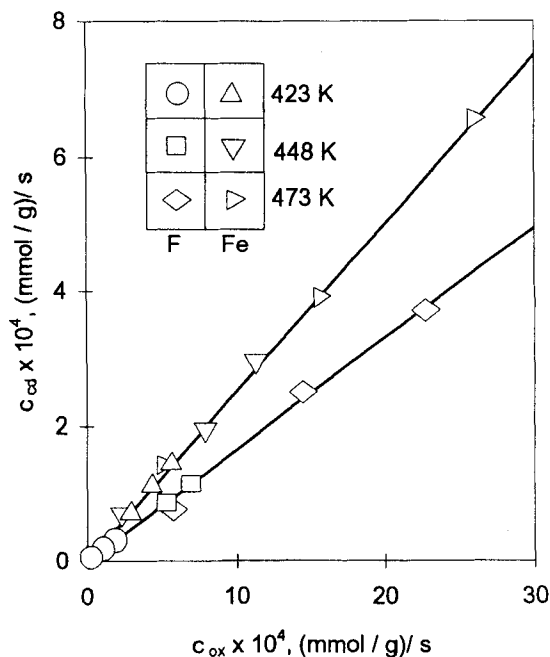


FIGURE 3 Correlation between the rates of carbon dioxide release ( $\dot{c}_{cd}$ ) and oxygen uptake ( $\dot{c}_{ox}$ ) in the stationary stage of oxidation of polyethylene layers of various thicknesses at different contact temperature in contact with steel (Fe) and Teflon (F).

of contact time which correspond to maximum magnitudes of these parameters decrease with rising contact temperature and decreasing thickness of the layer (Table II).

The constants of Equation (3) were obtained graphically by constructing plots of the calculated  $\dot{c}_{ox}|_{x=0}$  values for a series of selected  $k^*$  values. The plots for all three  $b$  values intersect at one common point. This allows one to determine directly both constants:  $\dot{c}_{ox}|_{x=0}$  and  $k^*$  (see Tables II and III). Figure 4 shows reasonable consistency of the calculated and experimental data.

The constants of Equation (3) were determined also for other parameters  $P$  which characterize contact thermooxidation, taking into account the linear relation between  $\dot{c}_{ox}$  and the respective rates of change of these parameters (Tables II and III). The experimental data fall on straight lines in coordinates  $\tanh(k^*b)P^{-1} = f(b)$  (for example see Fig. 4), thus showing their coincidence with the following equation analogous to Equation (3):

$$\dot{P} = \frac{\dot{P}_{x=0}}{k^*b} \tanh(k^*b) \quad (4)$$

where  $\dot{P}$ ,  $\dot{P}_{x=0}$  are the rate of change of parameters for a layer of definite thickness and for an infinitely thin layer, respectively, but  $k^* = (k/D)^{1/2}$ ;  $k$  and  $D$  are the effective rate constants of oxygen consumption and oxygen diffusion coefficient, respectively, re-

TABLE III  
Calculated values of constant  $k^*$  ( $\mu\text{m} \times 10^{-2}$ ) and  $b_{\text{crit}}$  ( $\mu\text{m}$ ) (numerator - steel, denominator - Teflon)

Parameter $\dot{P}$	Contact temperature, K					
	423		448		473	
	$k^*$	$b_{\text{crit}}$	$k^*$	$b_{\text{crit}}$	$k^*$	$b_{\text{crit}}$
$\dot{c}_{\text{ox}}$	1.76/0.97	5.7/10.3	1.92/1.29	5.2/7.8	2.10/1.80	4.8/5.6
$\dot{c}_{\text{od}}$	1.74/0.97	5.7/10.3	1.91/1.31	5.2/7.6	2.11/1.79	4.7/5.6
$D_{\text{og}}^*$	1.01	9.9	1.09	9.2	1.30	8.3
$\dot{A}$	0.83	12.0	0.85	11.8	0.91	10.9
$\Delta \dot{m}$	2.32	4.3	2.49	4.0	2.70	3.7

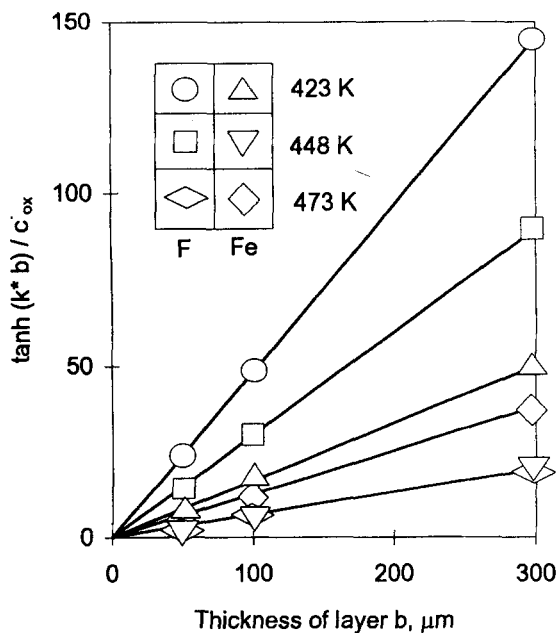


FIGURE 4 Variation of oxygen uptake rate,  $\dot{c}_{\text{ox}}$ , with thickness of polymer layer,  $b$ .

responsible for the change of the corresponding parameters  $P$  (in this stage of our studies it was possible to determine only the ratio of these values,  $k$ ).

The function  $\dot{A}(b)$  (see Tables II and III) correlates equally well with Equation (4). It means that the variation of rate of change of individual contact oxidation parameters,  $P$ , and also of  $A$  values with the thickness of the polymer layer,  $b$ , obey the same rule.

The values of  $k^*$  and  $\dot{P}_{x=0}$  increase with rising contact temperature (Tables II and III). On the basis of the data of Figures 4 and 5 the temperature dependence of these

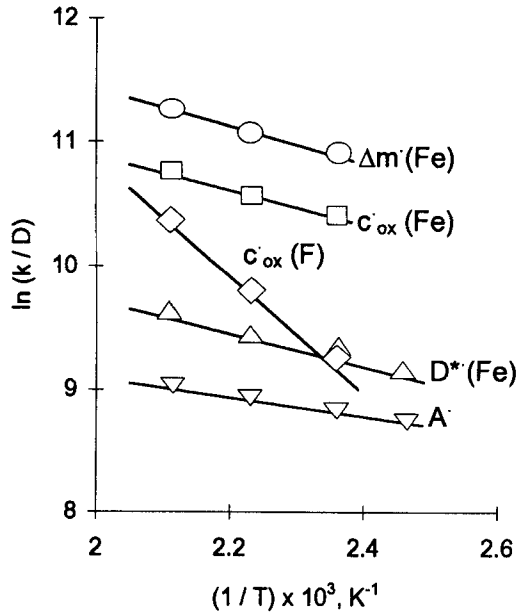


FIGURE 5 Temperature dependence of  $k/D$  ratio for different kinetic parameters.

characteristics can be described by conventional expressions:

$$k^{*2}(T) = \frac{k(T)}{D(T)} = \frac{k_0 \exp(E_0/RT)}{D_0 \exp(-E_D/RT)} = (k_0/D_0) \exp(-E_{k/D}/RT) \quad (5)$$

$$\dot{P}_{x=0} = P_{x=0} k(T) = P_{x=0} k_0 \exp(-E_0/RT) = \dot{P}_0^* \exp(-E_0/RT) \quad (6)$$

where  $k_0$ ,  $D_0$  and  $P_0$  are values of the respective characteristics at  $T^{-\infty}$ ;  $E_0$  is the effective energy of activation of contact oxidation conversions responsible for the change of the respective parameter,  $P$ ;  $E_D$  is the effective activation energy of oxygen diffusion;  $E_{k/D} = E_0 - E_D$ . The corresponding values of  $E$  were determined from the slopes of the plots of the respective parameters *versus* temperature (Figs. 5 and 6), and also the values of  $k_0/D_0$  and  $\dot{P}_0^*$  were calculated (Table IV).

Irrespective of the nature of the substrate used, the values of  $E_D$  were found to be very close. Obviously, kinetics of both contact oxidation and the change of  $A$  values is controlled by oxygen diffusion.

The values of  $E_0$  of polymer being oxidized on the steel surface in contrast to polymer on the Teflon surface are considerably lower (Table IV). This can be attributed to the catalytic effect of the steel surface. The rate of oxidation seems to be controlled by the content of iron compounds (mainly iron complexes with products of the oxidative destruction of polyethylene, containing carboxyl groups) which migrate into the bulk of polymer. Throughout the thickness of the layer the gradient of these compounds was observed.<sup>14</sup> It enables one to assume the existence of the respective gradient of oxidation rate constant.

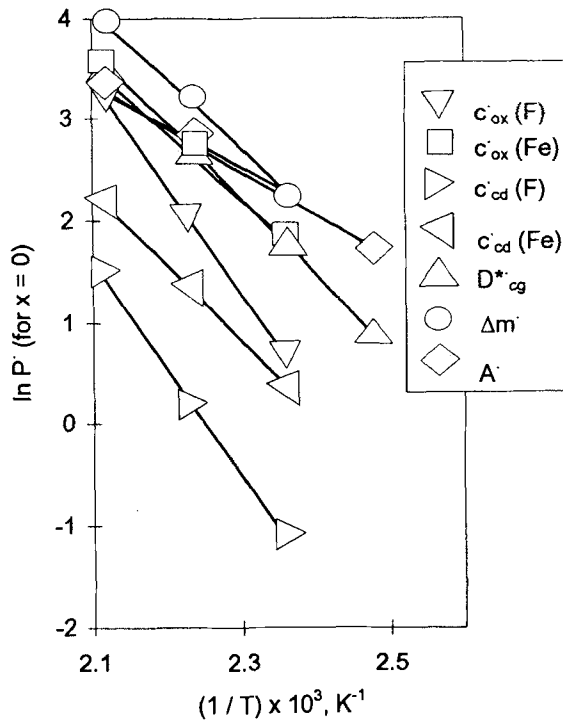


FIGURE 6 Temperature dependence of  $\dot{P}_{x=0}$  values for different parameters.

The shape of the  $A(t)$  curves is determined by the competitive effect of at least two trends of contact oxidation:<sup>7,15</sup> the accumulation of oxygen-containing groups and oxidative cross-linking causing the decrease of  $A$  values (process I),\* and reactions of oxidative destruction causing the decrease of  $A$  values (process II). The appearance of the maximum on the  $A(t)$  curves suggests that the process I prevails only at the onset of contact.

These two tendencies of contact thermooxidation allows one to state that

$$A(t) = A_1(t) - A_2(t) \quad (7)$$

where  $A_1(t)$  and  $A_2(t)$  are the additive changes in  $A$  values as a result of processes (I) and (II), respectively.

The chemical changes in a thin boundary layer during contact thermooxidation have the decisive effect on  $A$  values. A sufficiently high degree of contact oxidation conversion of adhesive in the boundary layer is attained comparatively early (as evidenced, for example, by the kinetics of the surface energy variation in the boundary layer<sup>17</sup>) and the oxidation process proceeds at a gradually diminishing rate. This is why

\* In Reference 16 we have shown that oxidative cross-linking plays the principal role in process I

TABLE IV  
 Values of constants of Eq. (5) and (6) (numerator - steel, denominator - Teflon)

Parameter	$E, \text{kJ/mol}$		$E_D$	unit	$\bar{P}_0^*$	$k_0/D_0, \mu\text{m}^{-2}$
	$E_0$	$E_{k/D}$				
$\zeta_{ox}$	60.7/90.8	10.9/39.3	49.8/51.5	(nmol/g)s <sup>-1</sup>	$1.5 \times 10^4/2.6 \times 10^7$	$6.7 \times 10^2/6.1 \times 10^8$
$\zeta_{ad}^*$	60.7/88.3	10.9/39.3	49.8/48.9	(mmol/g)s <sup>-1</sup>	$3.8 \times 10^3/2.1 \times 10^6$	$6.7 \times 10^2/6.1 \times 10^8$
$D_{eg}^*$	56.6	1.3	45.2	s <sup>-1</sup>	$5.0 \times 10^3$	$2.5 \times 10^5$
$\Delta \bar{m}$	55.6	10.5	45.2	mass parts <sup>-1</sup>	$6.1 \times 10$	$1.0 \times 10^6$
$A$	35.6	7.1	28.5	(N/m)s <sup>-1</sup>	$2.1 \times 10^5$	$5.1 \times 10^4$

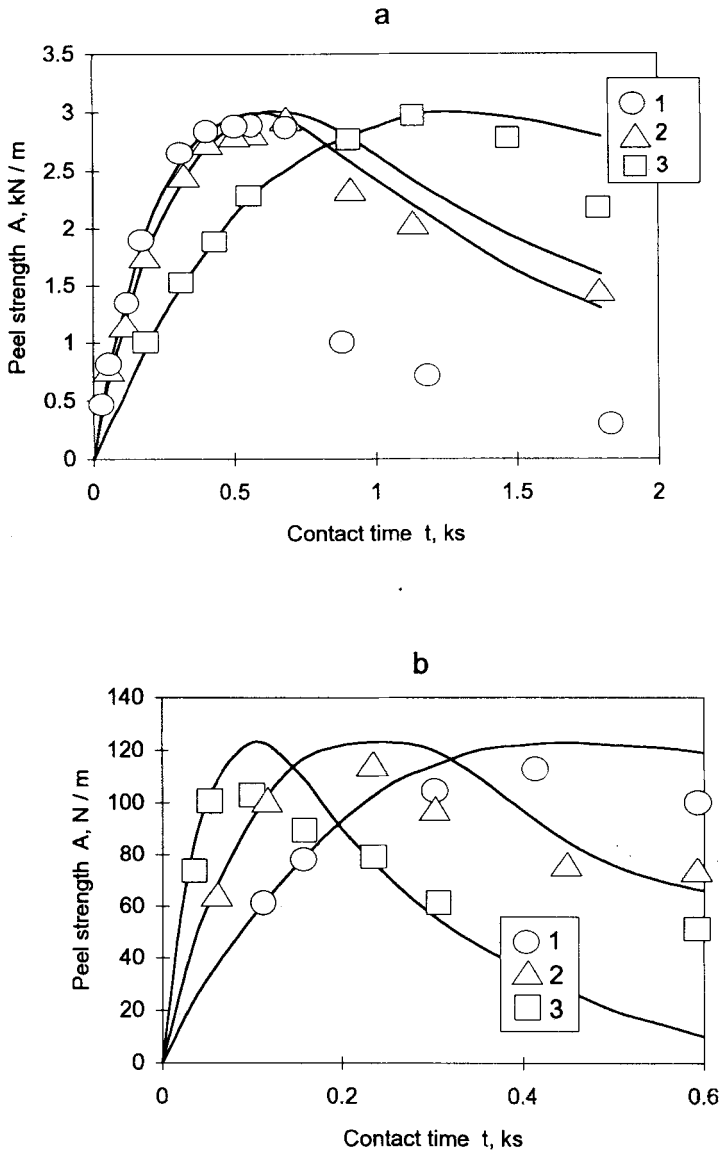


FIGURE 7 Experimental points and calculated  $A(t)$  curves: (a) for an open adhering system,  $b$  values ( $\mu\text{m}$ ): 1–50, 2–100, 3–300;  $T = 448$  K; (b) for a closed adhering system,  $b = 500$  mm;  $T$  values ( $^{\circ}\text{K}$ ): 1–423, 2–453, 3–483.

we specify the simplest asymptotic function satisfying this requirement, namely, the exponential function (corresponding to a first-order process):

$$A_1(t) = A_{\infty 1} [1 - \exp.(-k_1 t)] \tag{8}$$

$$A_2(t) = A_{\infty 2} [1 - \exp.(-k_2 t)] \tag{9}$$

Bearing in mind that at sufficiently large values of contact time the  $A(t)$  function tends to zero (Fig. 7),  $A_{\infty 1} = A_{\infty 2} = A_{\infty}$  and, in accordance with (7):

$$A(t) = A_{\infty} [\exp(-k_2 t) - \exp(-k_1 t)], \tag{10}$$

where  $k_1$  and  $k_2$  are the rate constants of the change in  $A$  values as a result of contact oxidation processes (I) and (II), respectively;  $A_{\infty}$  is the value of  $A$  at the completion of the process.

The  $A$ ,  $A_1$  and  $A_2$  contact time functions are shown in Figure 8. The  $A(t)$  function, Equation (10), is characterized by a sharp reduction in the growth rate for  $0 < t < t_{Amax}$ :

$$dA/dt = A_{\infty} [k_1 \exp(-k_1 t) - k_2 \exp(-k_2 t)] \tag{11}$$

The maximum growth rate  $A$  corresponds to  $t = 0$ :

$$A_{t=0} = \lim_{t \rightarrow 0} dA/dt = \Delta k A_{\infty} \tag{12}$$

where  $\Delta k = k_1 - k_2$ .

The expression of  $t_{Amax}$  (the value of  $t$  corresponding to  $dA/dt = 0$ ) is written as follows (see Figure 8):

$$t_{Amax} = \ln \chi_k / \Delta k \tag{13}$$

where  $\chi_k = k_1/k_2$

Insertion of Equation (13) into (12) gives:

$$\dot{A}_{t=0} = A_{\infty} \ln \chi_k / t_{Amax} \tag{14}$$

The function  $\dot{A}_{t=0}^{-1}(t_{Amax})$  (data of Table I) is shown in Figure 9a. This function can be approximated by a straight line common to all experimental points, regardless of contact temperature and thickness of the polymer layer. It means that, in accordance

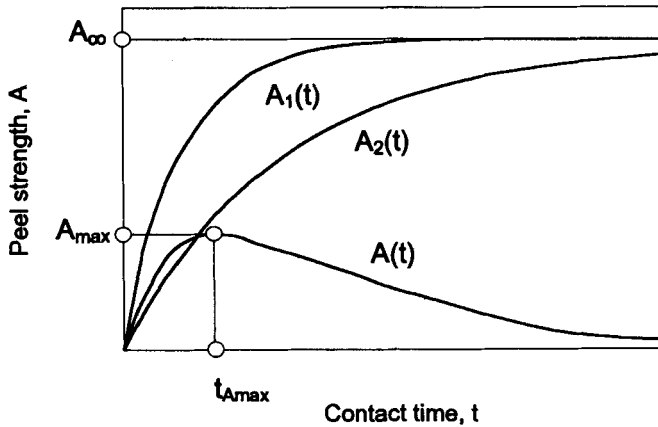


FIGURE 8 The shape of  $A_1(t)$ ,  $A_2(t)$  and  $A(t)$  functions calculated by Equations (8), (9) and (10), respectively.



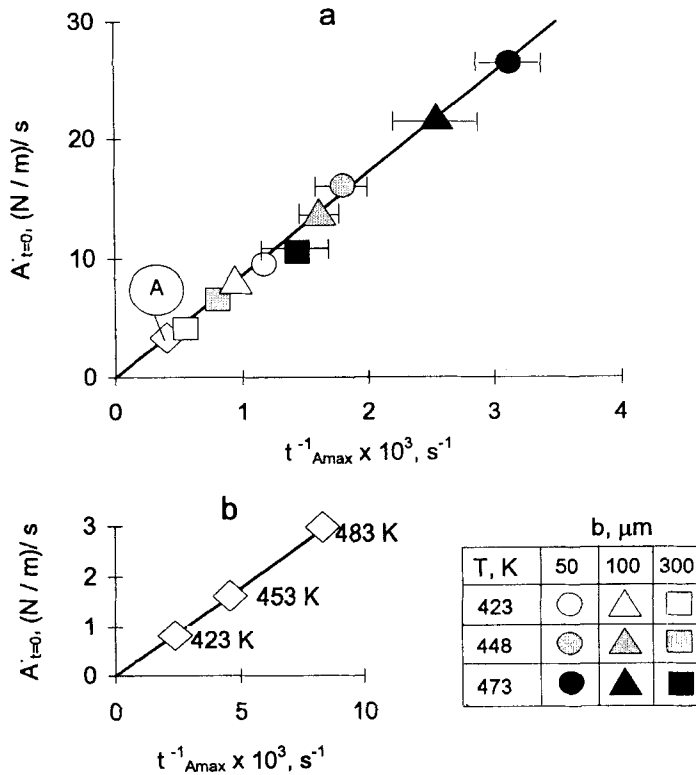


FIGURE 9 Correlation between  $A_{t=0}$  and  $t_{A_{\max}}$  values for open (a) and closed (b) adhering systems (the point A corresponds to  $T=453$  K and  $b=500$   $\mu\text{m}$ ).

with Equation (14),  $A_{\infty} \ln \chi_k = 8.50 \times 10^3$  N/m. Substituting (13) into (10), we obtain the expression for  $A_{A_{\max}}$  (Fig. 8):

$$A_{A_{\max}} = A_{\infty} [\exp(-\ln \chi_k / (\chi_k - 1)) - \exp(-\ln \chi_k / (1 - \chi_k^{-1}))] \quad (15)$$

In accordance with Equation (15), the  $A_{\max}$  value is determined only by  $A_{\infty}$  and  $\chi_k$ . The experimental values of  $A_{\max}$  differ slightly and, independently of the values of  $b$  and  $T$ , are within the limits  $(2.6 - 3) \times 10^3$   $\text{Nm}^{-1}$  (Fig. 7a). It means that  $A_{\max} = \text{constant}$ .

It follows from the condition  $A_{\infty} \ln \chi_k = \text{constant}$  (see Equations (14) and (15)) that  $A_{\infty}$  and  $\chi_k$  constants are independent of  $b$  and  $T$ . A similar conclusion can be drawn when we assume that  $A_{\infty}$  characterizes the state of equilibrium in the contact processes, whereas  $\chi_k$  is the ratio of rate constants. In the case when the effect of contact temperature on  $k_1$  and  $k_2$  is the same (see below), the  $\chi_k$  value also should be constant.

Thus, the kinetics of  $A(t)$  as a function of  $T$  and  $b$  must be determined by the type of  $k_1, k_2(b, T)$  functions. Now the values of  $A_{\infty}, k_1$  and  $k_2$  can be found which will satisfy Equation (11) and the experimental points of Figure 7a. It is impossible to determine them independently. To this end we used a program for computation of  $A(t)$  functions, Equation (11), for a series of  $A_{\infty} > 3 \times 10^3$   $\text{Nm}^{-1}$  and the respective values of  $k_1$  and  $k_2$

(the values of  $A_\infty < A_{\max}$  are senseless). Starting with  $A_\infty > 7 \times 10^3 \text{ Nm}^{-1}$ , the  $A(t)$  function depends slightly on  $A_\infty$ , whereas the calculated  $A_{\max}$  values become practically constant (Fig. 10, curve 2) and close to the experimental  $A_{\max}$  values.

In Figure 1, the  $A(t)$  curves calculated at  $A_\infty = 7 \times 10^3 \text{ Nm}^{-1}$  and  $\chi_k = 3.36$ , respectively, are shown as an example; while Table V gives the values of  $k_1$  and  $k_2$  constants. The experimental points fit satisfactorily with the calculated curves right up to  $A_{\max}$ . At  $t > t_{A_{\max}}$ , the experimental estimates of  $A$  are lower than the calculated ones. The higher the values of  $T$  and the lower the values of  $b$ , the more pronounced is this tendency. It could be explained as the effect of accumulation of macro-impurities (mainly of heterogeneous inclusions of low-molecular destruction products) in the boundary

TABLE V  
Constants of Equations (10) and (13) as function of contact temperature,  $T$ , and thickness of polymer layer,  $b$  (open adhering system),  $A_\infty = 7 \times 10^3 \text{ N/m}$ ;  $\chi_k = 3.96$ ;  $A_{\max} = 2.94 \times 10^3 \text{ N/m}$

$T, \text{K}$	$b, \mu\text{m}$	$k_1 \times 10^3, \text{s}^{-1}$	$k_2 \times 10^3, \text{s}^{-1}$	$\Delta k \times 10^3, \text{s}^{-1}$
423	0	1.91	0.57	1.34
	50	1.81	0.54	1.27
	100	1.58	0.47	1.11
	300	0.75	0.22	0.53
448	0	3.27	0.97	2.30
	50	3.11	0.92	2.19
	100	2.66	0.79	1.87
	300	1.28	0.38	0.90
473	0	5.71	1.70	4.01
	50	5.32	1.58	3.74
	100	4.53	1.35	3.18
	300	2.09	0.62	1.47

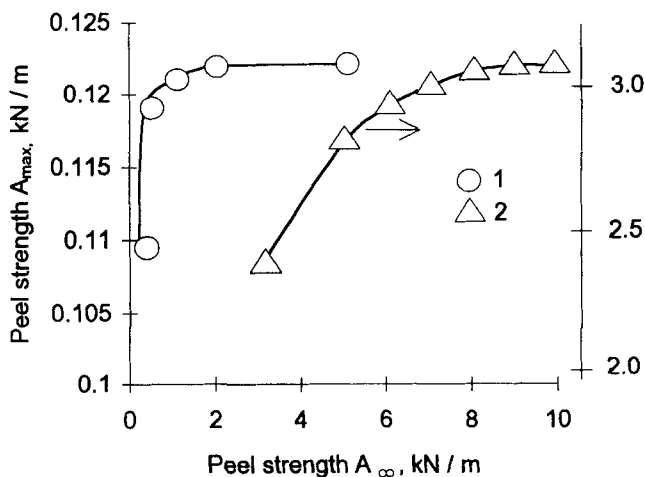


FIGURE 10 The dependence of the calculated  $A_{\max}$  values on the chosen  $A_\infty$  values for closed (1) and open (2) adhering systems.

layer, thus causing its weakening (these effects are, naturally, disregarded in Equation (11)).

The  $k_1$  and  $k_2$  values vary as a function of  $b$  and  $T$  (Table V). It follows from Equation (4) that

$$\dot{A}_{t=0}(b, T) = [\dot{A}_{t=0|b=0}(T)/k^*(T)b] \tanh(k^*b) \quad (16)$$

where  $\dot{A}_{t=0|b=0} = \lim_{b \rightarrow 0} \dot{A}_{t=0}(b)$

According to Equation (12) we can write:  $\dot{A}_{t=0}(b, T) = \Delta k(b, T)A$ ;  $\dot{A}_{t=0|b=0} = \Delta k_0(T)A_\infty$ ;  $\Delta k_0 = \lim \Delta k(b)$ , and after substitution into Equation (16) we obtain

$$\Delta k(b, T) = [k_0(T)/k^*(T)b] \tanh(k^*b) \quad (17)$$

where  $k^* = [k_0(T)/D(T)]^{1/2}$ .

Equations (16) and (17) are identical and the values of  $k^*$  are the same (Table III). The function  $\Delta k_0(T)$  (Figure 11) is characterized by the effective activation energy  $E_0$ , its value being close to the  $E_0$  for the temperature dependence of  $\dot{A}_{t=0}$  (Table IV). The linear shape of function  $\Delta k_0(T)$  in Arrhenius coordinates (Fig. 11) proves that the  $\Delta k_0, k_{01}, k_{02}$  as functions of temperature are characterized by the same value of  $E_0$  (Fig. 11).

Regardless of the formal character of the expressions obtained, their analysis gives important information about the possibilities to control the contact oxidation pro-

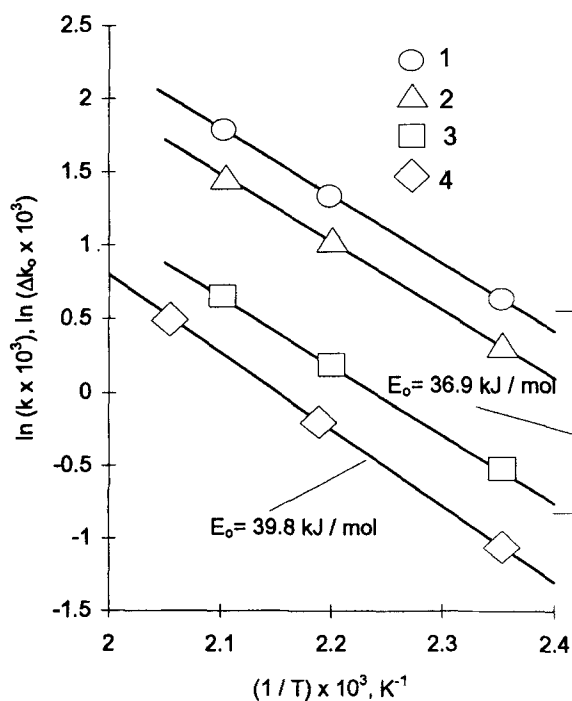


FIGURE 11 Temperature functions of constants of Equations (10, 11): 1— $k_{01}$ , 2— $\Delta k_0$ , 3— $k_{02}$  (an open system); 4— $\Delta k_0$  (a closed system).

TABLE VI  
 Constants of Equations (10) and (13) and some other kinetic characteristics of function  $A(t)$  for a closed adhering system;  $A_\infty = 2 \times 10^3$  N/m,  $\chi_k = 1.18$ ,  $A_{\max} = 120$  N/m

$T, K$	$k_1 \times 10^3, s^{-1}$	$k_2 \times 10^3, s^{-1}$	$\Delta k \times 10^3, s^{-1}$	$\dot{A}, (N/m)s^{-1}$	$t_{A_{\max}}, s$
423	2.29	1.94	0.35	0.7	470
453	4.59	3.89	0.70	1.4	236
483	9.83	8.33	1.50	3.0	110

cesses. The practical objectives are to accelerate the formation of adhering systems and to attain high values of  $A$ .

The possibilities to control the  $A(t)$  functions for a certain polymer-metal adhering system are restricted, since the characteristics  $\chi_k$ ,  $A_\infty$  and  $A_{\max}$  are constant. The process can be only enhanced (for  $t > t_{A_{\max}}$  and  $A < A_{\max}$ ) by increase of  $\Delta k$  ( $b$ ,  $T$ ) (growth of  $T$ ) and decrease of  $b$  values.

Equation (11) can be satisfactorily used to describe the  $A(t)$  function also in the absence of oxygen penetration through the polymer layer (oxygen trapped on the interface takes part in the contact oxidation),<sup>7</sup> for instance, see Figure 7b. The absolute values of constants in Equation (11) differ for open (polymer-metal) and closed (metal-polymer-metal) adhering systems (Tables II and VI). The  $A(t)$  function for a closed system is characterized by a low value of  $A_{\max}$ . This is due to the reduced oxygen amount accounting for the  $A_\infty$  value ( $A_\infty$  for closed adhering systems is about 0.3 of  $A_\infty$  for open adhering systems) and due to the decrease in  $\chi_k$  value. The values of  $\Delta k$  for closed adhering systems are higher, evidently, as a result of the specific effect of oxygen entrapped at the interface.<sup>7</sup> Moreover, the unfavorable conditions of escape of low-molecular weight oxidation products can adversely affect the  $A(t)$  functions for a closed adhering system; as a result the contribution of processes (II) should increase.

The potentiality of various polymer-metal systems is defined by  $A_{\max}$ . In accordance with Equation (16) an increase in  $A_{\max}$  values can be gained by increasing  $A_\infty$  and  $\chi_k$ , in other words, by increasing the yield of the processes (I) and also the ratio of rate constants for processes (I) and (II), respectively.

In conclusion, it should be emphasized that the observed regularities make it possible, to a certain extent, to predict the  $A(t)$  function. At the present stage of research the constants  $k_1$ ,  $k_2$ ,  $k^*$  and  $A_\infty$  should be regarded as empirical. Therefore, for the specified polymer-metal system it is necessary to evaluate experimentally the  $A(t)$  function right up to  $A_{\max}$  at one value of  $T$  and several  $b$  values;  $\chi_k$  and  $A_\infty$  can be determined from Equation (12);  $\Delta k$ ,  $k_1$  and  $k_2$  from Equations (13) and (12); and  $\Delta k_0$  from Equation (17). The values of  $\Delta k$ ,  $k_1$  and  $k_2$  can be calculated for any other value of  $T$  and  $b$ .

## CONCLUSIONS

The parameters characterizing contact thermoxidation process (the quantity of oxygen consumed, carbon dioxide released, carbonyl group content and the changes in weight of adhesive layer) are kinetically interrelated with the changes in peel strength ( $A$ ).

The kinetics of changes in  $A$  are completely defined by the kinetics of contact oxidation.

The dependence of the rate of changes in individual parameters of contact oxidation, and in values of  $A$ , the thickness of the adhesive layer and contact temperature can be described by a simple expression. The analysis of the constants of this expression enables one to evaluate quantitatively the extent of the catalytic effect of the substrate on contact oxidation process.

Peel strength-contact time relationships of an adhering system polyethylene-steel can be fairly well described by an expression comprising the effective rate constants of two competitive processes: the accumulation of oxygen-containing groups and oxidative cross-linking (I), and oxidative destruction (II).

### Acknowledgement

We appreciate financial support of this study by the Latvian Research Council (Grant for Project 93-0499).

### References

1. L. J. Malers, G. A. Zelcermains, A. V. Viksne, M. M. Kalnins, *Vysokomolekulyarnye Soedineniya, Seriya A*, **13** (3), 551 (1975).
2. L. J. Malers and M. M. Kalnins, *Vysokomolekulyarnye Soedineniya, Seriya A*, **18** (5), 1061 (1976).
3. M. M. Kalnins, J. J. Avotins, *Mechanics of Composite Materials*, **25** (6), 1031 (1989).
4. I. V. Kuleshov, S. I. Kaibin, M. M. Kalnins, *Vysokomolekulyarnye Soedineniya, Seriya B*, **25** (5), 366 (1983).
5. G. M. Bartenev, I. V. Kuleshov, M. M. Kalnins, S. I. Kaibin, *Doklady Akademii Nauk SSSR, Seriya Chem.*, **272** (6), 1418 (1983).
6. J. J. Bikerman, *J. Adhesion*, **3**, 333 (1972).
7. M. M. Kalnins, *Adhesive Interaction of Polyethylene with Steel* (Zinatne Publ., Riga, Latvia, 1990), Chap. 3, pp. 105-156.
8. M. M. Kalnins, *J. Adhesion*, **35**, 173 (1991).
9. D. E. Packham, in *Developments in Adhesives - 2*, A. J. Kinloch, Ed. (Applied Science Publ. Ltd., England, 1981), p. 315.
10. J. J. Malers, M. M. Kalnins, *Latvijas Zinatnu Akademijas Vestis, Kim. serija*, **6**, 654 (1979).
11. I. Crank, *The Mathematics of Diffusion*, 2nd ed. (Clarendon Press, Oxford, 1975), pp. 241-243.
12. N. C. Billingham, T. X. Walver, *J. Polymer Sci., Polymer Chem. Ed.*, **13** (6), 1209 (1975).
13. E. Kovacs, Z. Wolksber, *JUPAC Preprints*, **5**, 389 (1969).
14. M. M. Kalnins, J. J. Malers, *Latvijas Zinatnu Akademijas Vestis, Kim. serija*, **2**, 166 (1985).
15. M. M. Kalnins, *Proc. ACS, PMSE Div. Preprints*, **67**, 47 (1992).
16. M. M. Kalnins and J. L. Ozolins, *Mechanics of Composite Materials*, **20** (2), 201 (1984).
17. M. M. Kalnins, *Mechanics of Composite Materials*, **26** (5), 789 (1990).